

Optimization of Nano-Enhanced Elastomeric Adhesives through Combined Experimental and Computational Methods

Demetrios A. Tzelepis¹, Robert Hart, PhD¹,

¹US-ARMY CCDC-GVSC, Warren MI

ABSTRACT

Additions of both carbon fiber (CF) and carbon nano-tubes (CNTs) as reinforcements to polyurea (PUr) based adhesives are computationally investigated. Both CF and CNTs show an increase in stiffness. The effect of CF reinforcements on the PUr is more pronounced than the CNT's but this due to CNT loading being dramatically lower. On percent basis the CNT effect on strength was greater than the CF. Increasing hard segment content of PUr also had a positive effect on the joint strength, but a negative effect on the shear joint displacement. Finally the addition of CF reinforcements moved the performance of a PUr formulation from a Group IV adhesive into the Group III category. This paper illustrates the potential for commonly available reinforcements to be used to tailor the strength elongation characteristic of a PUr adhesive system.

Citation: Demetrios A. Tzelepis, Robert Hart, "Optimization of Nano-Enhanced Elastomeric Adhesives Through Combined Experimental and Computational Methods, In *Proceedings of the Ground Vehicle Systems Engineering and Technology Symposium (GVSETS)*, NDIA, Novi, MI, Aug. 13-15, 2019.

1. INTRODUCTION

Ground Vehicle Systems Center Engineers are evaluating the use of multiple material classifications, such as high strength aluminum, advanced high strength steel alloys along with various composites and ceramics in combat vehicle designs. This inevitably leads to multi-material joints, wherein fusion welding processes are not possible, or will lead to inadequate joining efficiency. Adhesive bonding offers an alternative

to fusion welding. Jensen et al. classifies adhesive joints into four categories based on their strengths and elongations at failure [1] and [2]. He further describes how adhesives that have high strength exhibit low elongations to failure and conversely adhesives with high elongations exhibit low strengths, both of which demonstrate poor damage tolerance traits for Army applications. In other words, there is a need for adhesives that have excellent stiffness-toughness balance as indicated by Group I, Figure 1.

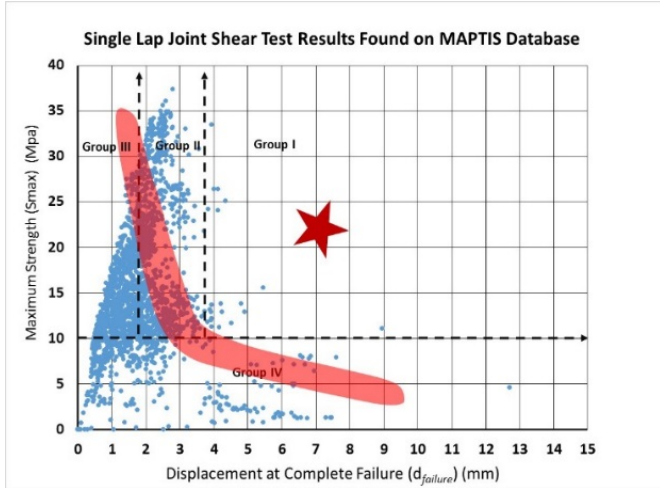


Figure 1- Results from single lap joint testing of various commercially available adhesives from NASA MAPTIS database

There are two primary approaches to achieving the desired outcome. The first is to modify or toughen existing high strength-low ductility adhesives (thermoset and thermoplastic type adhesives) and the second is to strengthen high ductility-low strength adhesives (elastomeric adhesives). This paper follows the second approach by optimizing the strength and elongation characteristics of polyurea (PUr) adhesives through the addition of reinforcements at multiple length-scales, from nano- to milli- scales.

Polyurea (PUr) elastomeric coatings have been used and studied as blast mitigation technology for several years [3]. Typically, PUr is formed from the reaction of two organic molecules, isocyanate and amine; this results in a phase segmented nano-scale microstructure, consisting of hydrogen bonded hard segment/domains (high Tg) and soft segments/domains (low Tg) [4]. Grucjic et al. showed shock loading of PUrs causes extensive hydrogen bond breaking and this hydrogen bond is associated with substantial energy absorption observed in high blast/ballistic impact mitigation. [5]. Fragiadakis et. al, showed small changes in hard segment content can have dramatically

different mechanical response, from a deformable soft rubber to a rigid brittle material [6].

Their unique mechanical response at high strain rates show that there is potential in development of novel adhesives, but to be used as a structural adhesive the strengths and stiffness would most likely have to increase.

Nano-particle reinforcements is one potential path in strengthening PUr for the purpose of being used as a structural adhesive. Experimental and multiscale modeling studies have shown that carbon nanotubes provide crack-bridging capabilities within a polymer matrix, which effectively increase the strength of the nanocomposite [7]. X.Qian et al. showed that 80% improvement in strength with no significant loss in elongation when using 0.2 wt% graphene reinforcement, while Graphite Oxide provided no significant improvement in properties. [8] Cai and Song showed the addition of a Cloisite® 20A (dimethyl dehydrogenated tallow quaternary ammonium(2M2HT-MMT) improved the Young's modulus, fracture strength at break, and elongation at break were improved by 40%, 110% and 50% respectively [9]. In addition to mechanical advantages, carbon nanotube reinforcements have potential to optimize thermal and electrical properties, which may be advantageous in controlling thermal management or for electrically grounding materials through the joint interface [10].

The use of nano-reinforcements and control in the HS-SS ratios in PUr's could provide a tailored approach to developing structural adhesives from elastomeric based coatings.

2. EXPERIMENTAL

2.1. Raw Materials

The PUr formulation is based on an Isophorone diisocyanate (IPDI) chemistry. IPDI-Vestanat was

obtained from Evonik Corporation. Jeffamine T5000 and D2000 polyetheramines were obtained from the Huntsman Corporation. The diethyltoluene diamine (DETDA) (Lonzacure) was obtained from Lonza. Single-walled carbon nanotubes (SWCNT's) were obtained from Sigma Aldrich (CAS: 308068-56-6) and had the following salient properties: 1.3-2.3 nm in diameter, 1µm in length, 600 GPa modulus. T700 Carbon Fibers (Toray), were used and had properties of: 12k tow, 7 µm filament diameter, 6-25mm length, 230 GPa modulus.

2.2. Preparation of PUr's and PUr's/composites.

An isocyanate prepolymer (A-side) was prepared by reacting the IPDI with 1:4 ratio by weight of triamines (T5000) to diamines (D2000). The reaction was carried out in a double walled bench-top 500 ml reactor under vigorous agitation. The IPDI was placed in the reaction vessel, and the amine mixture was added dropwise. The B-side was a mixture of DETDA and Triamines. Concentrations of the DETDA and Triamines, along with the A-side %NCO were varied in order to achieve an approximate 20, 30 and 40 percent hard content. Table 1 summarizes the PUr compositions.

Table 1 -

	IPDI-1	IPDI-4	IPDI-20
A-Side %NCO	12.8	8.7	17.0
% Hard Content	31 %	22 %	41 %

The carbon fiber and SWCNT's were added to the B-Side and mechanically mixed for 20 minutes. In addition, the SWCNT's were pulse ultrasonically stirred for a total energy of 70 kJ.

25 ml of the A-side and 25 ml of the B-side were placed in a two-component adhesive cartridge. A

3-inch 12 element static mixing was attached to the cartridge and pneumatic applicator along with a thick film applicator which was used to create 2 mm thick PUr film on a Teflon sheet.

3. COMPUTATIONAL MODELING

Computational models of the novel PUr adhesives were developed to simulate the influence of carbon fiber (CF) and carbon nanotubes (CNTs). First, the experimental tensile results of the three PUr formulations (IPDI-1, IPDI-4, IPDI-20) were used to develop an elastic-plastic material model in the multiscale modeling software package MultiMechanics. The elastic modulus, yield strength, kinematic and isotropic hardening moduli, and isotropic hardening exponent were extracted from experimental tensile curves. The elastic modulus was determined from the slope of the initial linear portion of the stress-strain curve. Yield strength was determined as the point where the linear region transitions to a rounded curve. The kinematic modulus was determined as the slope of the second linear portion after yield. The isotropic modulus and exponent were determined by fitting a power curve to the rounded curve just after the yield point of the material. Once the material parameters were determined for each PUr formulation, a representative volume element (RVE) of each material was subjected to a virtual tensile test, and the stress and strain were recorded in the same way as an experimental tensile test. Once the computational models were confirmed to accurately represent experimental results, the next step was to determine the influence of reinforcements on the response of the PUr adhesive systems.

Using the MultiMechanics software, additional RVE's were created with 0.001% CNTs, 0.01% CNTs, 1% CF, 5% CF, and 10% CF. Due to the high aspect ratios of both CNTs and CFs, these reinforcements were modeled as 1-D bar elements within the 3-D RVE. This strategy was utilized to increase computational efficiency as it becomes highly inefficient to model long filaments as 3-D

structures due to the need for extremely fine meshing. The CNTs were assigned a diameter of 2.3 nm with 1 μm length, whereas the CFs were modeled in bundles of 12,000 fibers each (12k tow). The 12k tow, made up of 7 μm diameter fibers, was modeled as bundles with 0.766 mm diameter and 25 mm length. The RVEs were used to develop homogenized properties of the CNT and CF reinforced adhesives, and these homogenized properties were used to develop stress-strain curves using a virtual tensile test. In total, 15 stress-strain curves were developed in Multi-Mechanics for each of the three PUR formulations (IPDI-1, IPDI-4, IPDI-20) with 5 different reinforcement alternatives (no reinforcement, 0.001% CNT, 0.01% CNT, 1% CF, 5% CF, 10% CF). The computational stress-strain curves are displayed alongside experimental results in Figure 2.

The computational stress-strain curves from MultiMechanics were used to model the PUR adhesives in a single-lap shear test in Abaqus CAE. In Abaqus CAE, the PUR materials were treated as an elastic-plastic material with 3-D quadratic hex elements. Taking advantage of symmetry, only half of the single lap shear joint was modeled. A displacement boundary condition was placed on the aluminum substrate to simulate a tensile test, and the lap shear joint was tested until the adhesive failed. For each adhesive model the displacement at failure was recorded, and the maximum effective joint strength was determined by dividing the force by the adhesive bond area, shown in Figure 4.

4. RESULTS AND DISCUSSION

Observing the experimental and computational stress-strain curves in Figure 2, the influence of the CNT and CF reinforcements become apparent. The most obvious takeaway is that for all three PUR formulations, the 1%, 5%, and 10% CF reinforcements resulted in significantly higher stiffness and strength compared to the original, unreinforced adhesives.

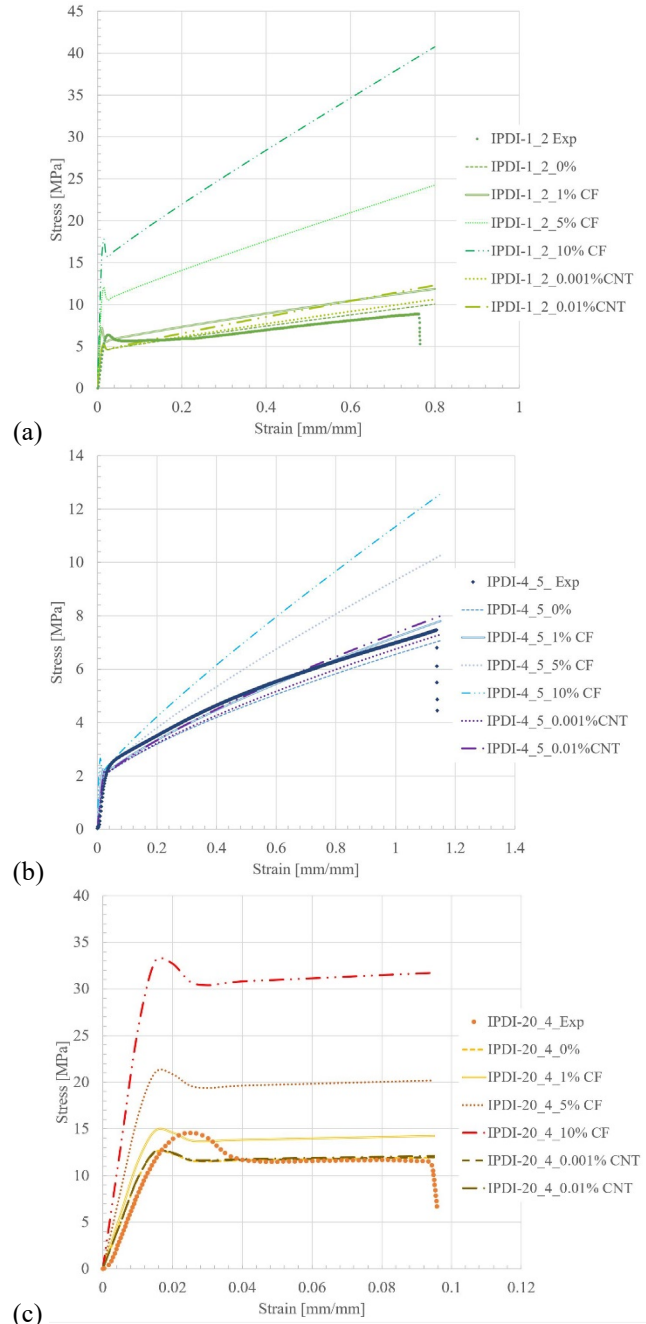


Figure 2- Experimental and computational tensile results for three PUR adhesives with and without carbon fiber and carbon nanotube reinforcements

The 0.001% and 0.01% CNT adhesives were also stiffer and stronger than the neat adhesive, however the influence was less pronounced compared to the CF adhesives. This trend was more of an artifact of

the percentages of the respective reinforcements than it was on the CFs and CNTs themselves. On a percentage basis, there was approximately 1000 times more CFs in the adhesive models that there were CNTs, but on a normalized basis, the CNTs actually had greater effect on the adhesive properties than the CFs.

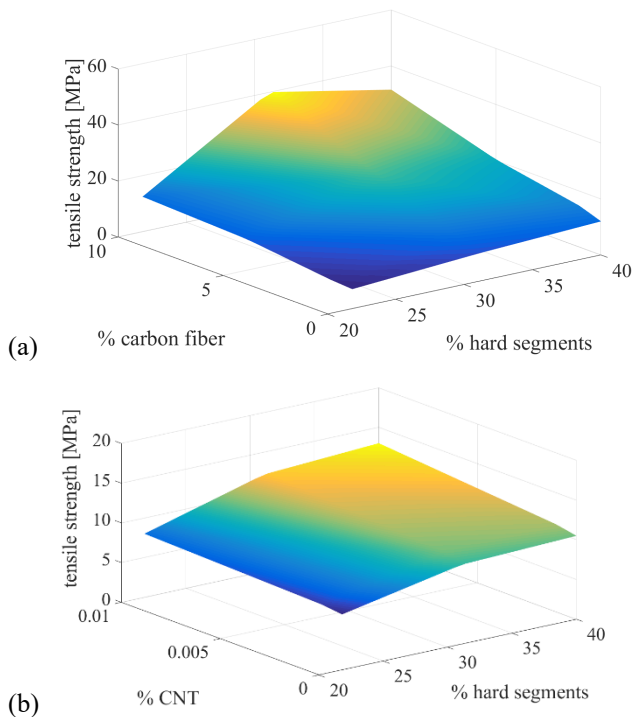


Figure 3- Surface plots of adhesive tensile strength as a function of the percentages of hard segments and (a) carbon fibers and (b) carbon nanotubes

The surface plots in Figure 3 illustrate the influence of both the adhesive formulation and reinforcements on the tensile strength of the adhesive systems. As seen in Figure 3 (a), as the percentage of CFs increased, the tensile strength increased accordingly. Similarly, as the percentage of CNTs increased there was a corresponding increase in tensile strength. In addition to the reinforcements, the percentage of hard segments in each of the adhesive formulations had a significant influence on the strength of the adhesive system. As the percentage of hard segments increased, the

strength of the adhesive system increased as well. In viewing the surface plots, one can see that in order to maximize strength of the adhesive, an optimum adhesive would have higher reinforcement content and higher hard segment content. It should be noted however that results cannot be extrapolated beyond the surface shown in Figure 3. There is a ceiling in the feasible reinforcement and hard segment content, which is not known at this time and is out of scope for the current study. While strength was positively influenced by increased hard segment content, the single lap shear joint displacement, shown in Figure 4, was negatively impacted by increased hard segment content

As seen in Figure 4, the PUr formulation IPDI-4, had the lowest hard segment content, but showed the highest displacement at failure. The formulation IPDI-1, which had an intermediate hard segment content experienced less displacement at failure, but did have a higher maximum effective joint strength. A noteworthy takeaway was that the CF reinforcements had a dramatic effect on the maximum effective joint strength of formulation IPDI-1. As observed in Figure 4, the addition of the CF reinforcements moved the performance of the IPDI-1 formulation from a Group IV adhesive up into the Group III category. In addition both CF and CNT reinforced adhesives experienced larger displacements at failure compared to un-reinforced adhesives. These results illustrate the potential to use commonly available reinforcements to tailor the strength and elongation characteristics of an adhesive system, and may provide a basis for future application-based optimization of adhesive systems.

